

Learning same-different relations strains feedforward neural networks

Junkyung Kim† Matthew Ricci† Thomas Serre

†equal contributions

*Department of Cognitive, Linguistic & Psychological Sciences
Brown Institute for Brain Science
Brown University, Providence, RI 02912, USA.*

1 **Abstract**

2 Progress in deep learning has recently led to great successes in many engineering applications
3 (LeCun et al., 2015). As a prime example, convolutional neural networks (CNNs), a type of
4 feedforward neural network, are already approaching human accuracy on visual recognition tasks
5 including object categorization (He et al., 2015) and face recognition (Kemelmacher-Shlizerman
6 et al., 2016). Here, we show that feedforward neural networks struggle to learn abstract visual
7 relations that are otherwise effortlessly recognized by non-human primates (Donderi and Zelnicker,
8 1969; Katz and Wirght, 2006), birds (Daniel et al., 2015; Martinho III and Kacelnik, 2016), rodents
9 (Wasserman et al., 2012) and even insects (Giurfa et al., 2001). We systematically study the ability
10 of feedforward neural networks to learn to recognize a variety of visual relations and demonstrate
11 that same-different visual relations pose a particular strain on these networks. Networks fail
12 to learn same-different visual relations when rote memorization becomes impossible (as when
13 stimulus variability exceeds their effective capacity). The comparative success of biological neural
14 networks in learning visual relations suggests that feedback mechanisms such as attention, working
15 memory and perceptual grouping are the key components underlying human-level abstract visual
16 reasoning.

17 **Keywords:** Visual Relations; Visual Reasoning; Convolutional Neural Networks; Deep Learning;
18 Working Memory; Visual Attention

19 **Introduction**

20 Consider the images on Figure 1(a). These images were correctly classified as two different breeds
21 of dog by a state-of-the-art computer vision system called a deep “convolutional neural network”
22 (CNN; He et al., 2015). This is quite a remarkable feat because the network must learn to extract
23 subtle diagnostic cues from images subject to wide variability of factors such as scale, pose and
24 lighting. The network was trained on millions of photographs, and images such as these were
25 accurately categorized into one thousand natural object categories, surpassing, for the first time,
26 the accuracy of a human observer for the recognition of one thousand image categories on the
27 ImageNet classification challenge.

28 Now, consider the image on the left side of Figure 1(b). On its face, it is quite simple compared
29 to the images on Figure 1(a). It is just a binary image containing two three-dimensional shapes.
30 Further, it has a rather distinguishing property: both shapes are the same up to rotation. The
31 relation between the two items in this simple scene is rather intuitive and obvious to a human
32 observer. Moreover, the ability to detect visual sameness is not unique to humans. In a striking
33 example from Martinho III and Kacelnik (2016), newborn ducklings were shown to imprint on an
34 abstract concept of “sameness” from birth (Figure 1(b), right panel). Yet, as we will show in this
35 study, CNNs struggle to learn this seemingly simple concept.

36 Why is it that a CNN can accurately categorize natural images while struggling to recognize a
37 simple abstract relation? That such task is difficult or even impossible for contemporary computer
38 vision algorithms like CNNs, is known. Previous work by Fleuret et al. (2011) has shown that

39 black-box classifiers fail on most tasks from the synthetic visual reasoning test (SVRT), a battery
40 of twenty-three visual-relation problems, despite massive amounts of training data. More recent
41 work has shown how CNNs, including variants of the popular LeNet (LeCun et al., 1998) and
42 AlexNet (Krizhevsky et al., 2012) architectures, could only solve a handful of the twenty-three
43 SVRT problems (Ellis et al., 2015; Stabinger et al., 2016). Similarly, Gülçehre and Bengio (2013),
44 after showing how CNNs fail to learn a same-different task with simple binary “sprite” items, only
45 managed to train a multi-layer perceptron on this task by providing carefully engineered training
46 schedules.

47 However, these results were inconclusive. First, each of these studies only tested a small number of
48 feedforward architectures, leaving open the possibility that low accuracy on some of the problems
49 might simply be a result of a poor choice of model hyper-parameters. Second, while the twenty-three
50 SVRT problems represent a diverse collection of visual relations, each problem has different image
51 features. Thus, the performance of a computational model on a given problem may be driven by
52 specific features in that problem, rather than the underlying abstract rule. To our knowledge, there
53 has been no systematic exploration of the limits of contemporary machine learning algorithms to
54 solve relational reasoning problems. Additionally, the issue has been overshadowed by the recent
55 success of novel architectures called “relational networks” (RNs) on seemingly challenging “visual
56 question answering” benchmarks (Santoro et al., 2017).

57 In this study, we probe the limits of feedforward neural networks including CNNs and RNs on
58 visual-relation tasks. In Experiment 1, we perform a systematic performance analysis of CNN
59 architectures on each of the twenty-three SVRT problems, which reveals a dichotomy of visual-relation

60 problems: hard same-different problems and easy spatial-relation problems. In Experiment 2, we
61 introduce a novel, controlled, visual-relation challenge called PSVRT, which we use to demonstrate
62 that CNNs solve same-different tasks only inefficiently, via rote memorization of all possible
63 spatial arrangements of individual items. In Experiment 3, we examine two models, the RN and a
64 novel Siamese network, which simulate the effects of perceptual grouping and attentional routing
65 to solve visual relations problems. We find that the former tends to overfit to particular item
66 features, but that the latter can render seemingly difficult visual reasoning problems rather trivial.

67 Overall, our study suggests that a critical re-appraisal of the capability of current machine vision
68 systems is warranted. We further argue that mechanisms for individuating objects and manipulating
69 their representations, presumably through feedback processes that are currently lacking in current
70 feedforward architectures, are necessary for abstract visual reasoning.

71 **Experiment 1: A taxonomy of visual-relation problems**

72 *The SVRT challenge*

73 The Synthetic Visual Reasoning Test (SVRT) is a collection of twenty-three binary classification
74 problems in which opposing classes differ based on whether or not images obey an abstract rule
75 (Fleuret et al., 2011). For example, in problem number 1, positive examples feature two items
76 which are the same up to translation (Figure 2), whereas negative examples do not. In problem 9,
77 positive examples have three items, the largest of which is in between the two smaller ones. All
78 stimuli depict simple, closed, black curves on a white background.

79 For each of the twenty-three problems, we generated 2 million examples split evenly into training

80 and test sets using code made publicly available by the authors of the original study at <http://www.idiap.ch/~fleuret/svrt>.
81

82 *Hyper-parameter search*

83 We tested CNNs of three different depths (2, 4 and 6 convolutional layers) and three different
84 convolutional receptive field sizes (2×2 , 4×4 and 6×6) for a total of nine networks. All networks
85 used pooling kernels of size 3×3 , convolutional strides of 1, pooling strides of 2 and three fully
86 connected layers. Pooling layers used ReLu activations. We trained all nine networks on each
87 problem and selected the best-performing network for each problem. All networks were trained
88 using the Adaptive Moment Estimation (Adam) optimizer (Kingma and Ba, 2015) with base
89 learning rate of $\eta = 10^{-4}$. All experiments were run using TensorFlow (Abadi et al., 2016).

Figure 2. *Examples images of twenty-three SVRT problems.* For each problem, three example
images, two negative and one positive, are displayed in a row. Problems are ordered and
color-coded identically to Figure 3. Images in each problem respect a certain structure (e.g., In
problem 9, three objects, identical up to a scale, are arranged in a row.). Positive and negative
categories are then characterized by whether or not objects in an image respect a rule (e.g., In
problem 3, an image is considered positive if it contains two touching objects and negative if
it contains three touching objects.). Descriptions of all problems can be found in Fleuret et al.
90 (2011).

91 *Results*

92 Shown in Figure 3 is a bar plot of the best-performing network accuracy for each of the
93 twenty-three SVRT problem (sorted by accuracy). Bars are colored red or blue according to the
94 SVRT problem descriptions given in (Fleuret et al., 2011). Problems whose descriptions have

95 words like “same” or “identical” are colored red. These *Same-Different* (SD) problems have items
96 that are congruent up to some transformation. *Spatial-Relation* (SR) problems, whose descriptions
97 have phrases like “left of”, “next to” or “touching,” are colored blue. Figure 2 shows positive and
98 negative samples for each of the corresponding twenty-three problems (also sorted by accuracy).
99 The resulting dichotomy across the SVRT problems is striking (Figure 3). CNNs fare uniformly
100 worse on SD problems than they do on SR problems. Many SR problems were learned
101 satisfactorily, whereas some SD problems (e.g., problems 20, 7) resulted in accuracy not
102 substantially above chance. From this analysis, it appears as if SD tasks pose a particularly
103 difficult challenge to CNNs. This result matches earlier evidence for a visual-relation dichotomy
104 hypothesized by Stabinger et al. (2016) which was unknown to us at the time of our own
105 experiments.

106 Additionally, our search revealed that SR problems are equally well-learned across all network
107 configurations, with less than 10% difference in final accuracy between the worst and the best
108 network. On the other hand, larger networks yielded significantly higher accuracy on SD problems
109 compared to smaller ones, suggesting that SD problems require a higher capacity than SR
110 problems. Experiment 1 corroborates the results of previous studies which found feedforward
111 neural networks performed badly on many visual-relation problems (Fleuret et al., 2011; Gülçehre
112 and Bengio, 2013; Ellis et al., 2015; Stabinger et al., 2016; Santoro et al., 2017) and suggests that
113 low accuracy cannot be simply attributed to a poor choice of hyper-parameters.

114 *Limitations of the SVRT challenge*

115 Though useful for surveying many types of relations, the SVRT challenge has two important
116 limitations. First, different problems have different image features. For instance, Problem 2
117 (“*inside-outside*”) requires that an image contain one large object and one small object. Problem 1
118 (“*same-different up to translation*”), on the other hand, requires that an image contains two items
119 identically-sized and positioned without one being contained in the other. In other cases, different
120 problems simply require different number of objects in a single image (two items in Problem 1
121 vs. three in Problem 9). Overall, this leaves open the possibility that image features, not abstract
122 relational rules, make some problems harder than others. Second, the ad hoc procedure used to
123 generate simple, closed curves as items in SVRT prevents quantification of image variability and
124 its effect on task difficulty. As a result, even within a single problem in SVRT, it is unclear whether
125 its difficulty is inherent to the classification rule itself or simply results from the particular choice
126 of image generation parameters unrelated to the rule. A better way to compare visual-relation
127 problems would be instead to define various problems on the *same* set of images.

128 **Experiment 2: A systematic comparison between spatial-relation and**
129 **same-different problems**

130 *The PSVRT challenge*

131 To address the limitations of SVRT, we constructed a new visual-relation benchmark consisting of
132 two idealized problems from the dichotomy that emerged from Experiment 1 (Figure 4): *Spatial*
133 *Relations* (SR) and *Same-Different* (SD). Critically, both problems in this new benchmark used
134 the exact same images, but with different labels. Further, we parameterized the dataset so that we

135 could systematically control various image parameters, namely, the size of scene items, the number
136 of scene items, and the size of the whole image. Items were binary bit patterns placed on a blank
137 background.

138 For each configuration of image parameters, we trained a new instance of a single CNN architecture
139 and measured the ease with which it fit the data. Our goal was to examine how hard it is for a CNN
140 architecture to learn relations for visually-different but conceptually-equivalent problems. For
141 example, imagine two instances of the same CNN architecture, one trained on a same-different
142 problem with small items in a large image, and the other trained on large items in a small image. If
143 the CNNs can truly learn the “rule” underlying these problems, then one would expect the models
144 to learn both problems with more-or-less equal ease. However, if the CNN only memorizes the
145 distinguishing features of the two image classes, then learning should be affected by the variability
146 of these features. For example, when the image and items are large, there are simply more possible
147 samples, which might slow down the training of a CNN trying to learn by rote memorization. In
148 rule-based problems such as visual relations, these two behaviors can be distinguished by training
149 and testing the same architecture on a problem instantiated over a multitude of image distributions.
150 There is no hold-out set in this experiment. Our main question is not whether a model trained
151 on one set of images can accurately predict the labels of another, unseen set of images sampled
152 from the same distribution. Rather, we want to understand whether an architecture that can easily
153 learn generalizable representations of one set of image parameters can also learn comparably
154 generalizable representations of another set of parameters with equal ease by taking advantage
155 of the abstractness of the visual rule.

156 *Methods*

157 Our image generator produces a gray-scale image by randomly placing square binary bit patterns
158 (consisting of values 1 and -1) on a blank background (with value 0). The generator uses three
159 parameters to control image variability: the size (m) of each bit pattern or item, the size (n) of
160 the input image and the number (k) of items in an image. These parameters allow us to quantify
161 the number of possible images in a dataset as $\mathcal{O}(P_{n^2,k} 2^{km^2})$, where $P_{a,b}$ denotes the number of
162 possible permutations of a elements from a set of size b . Our parametric construction allows a
163 dissociation between two possible factors that may affect a problem difficulty: classification rules
164 vs. image variability. To highlight the parametric nature of the images, we call this new challenge
165 the *parametric SVRT* or *PSVRT*.

166 Additionally, our image generator is designed such that each image can be used to pose both
167 problems by simply labeling it according to different rules (Figure 4). In SR, an image is classified
168 according to whether the items in an image are arranged horizontally or vertically as measured
169 by the orientation of the line joining their centers (with a 45° threshold). In SD, an image is
170 classified according to whether or not it contains at least two identical items. When $k \geq 3$, the
171 SD category label is determined by whether or not there are *at least 2* identical items in the
172 image, and the SR category label is determined according to whether the *average* orientation
173 of the displacements between all pairs of items is greater than or equal to 45° . Each image is
174 generated by first drawing a joint class label for SD and SR from a uniform distribution over
175 $\{Different, Same\} \times \{Horizontal, Vertical\}$. The first item is sampled from a uniform distribution
176 in $\{-1, 1\}^{m \times m}$. Then, if the sampled SD label is *Same*, between 1 and $k - 1$ identical copies of the
177 first item are created. If the sampled SD label is *Different*, no identical copies are made. The rest

178 of k unique items are then consecutively sampled. These k items are then randomly placed in an
179 $n \times n$ image while ensuring at least 1 background pixel spacing between items. Generating images
180 by always drawing class labels for both problems ensures that the image distribution is identical
181 between the two problem types.

182 We trained the same CNN repeatedly from scratch over multiple subsets of the data in order to see if
183 learnability depends on the dataset’s image parameters. CNNs were trained on 20 million images
184 and training accuracy was sampled every 200 thousand images. These samples were averaged
185 across 10 repetitions of each condition, yielding a single, scalar measure of learnability called
186 “average training accuracy” (ATA). In all of our experiments, accuracy either gradually increased
187 or saturated at some fixed value. Therefore, ATA is high only when accuracy increases earlier and
188 more rapidly throughout the course of training and if it converges to a higher final accuracy by the
189 end of training.

190 First, we found a baseline architecture which could easily learn both same-different and
191 spatial-relation PSVRT problems for one parameter configuration (item size $m = 4$, image size
192 $n = 60$ and item number $k = 2$). Then, for a range of combinations of item size, image size
193 and number of items, we trained an instance of this architecture from scratch. If a network
194 uses the first strategy when learning the problem, the resulting representations will be efficient at
195 handling variations unrelated to the relation (e.g., a feature set to detect *any* pair of items arranged
196 horizontally). As a result, the network should be equally good at learning the same problem in
197 other image datasets with greater intra-category variability. In other words, average accuracy will
198 be consistently high over a range of image parameters. Alternatively, if the network’s architecture

199 doesn't allow for such representations and thus is only able to learn prototypes of examples within
200 each category, the architecture will be progressively worse at learning the same visual relation
201 instantiated with higher image variability. In this case, average accuracy will gradually decrease
202 as image variability increases.

203 We varied each of three image parameters separately to examine its effect on learnability. This
204 resulted in three sub-experiments (n was varied between 30 and 180 while m and k were fixed
205 at 4 and 2, respectively; m was varied between 3 and 7, while n and k were fixed at 60 and 2,
206 respectively; k was varied between 2 and 6 while n and m were fixed at 60 and 4, respectively). To
207 use the same CNN architecture over a range of image sizes n , we fixed the actual input image
208 size at 180 by 180 pixels by placing a smaller PSVRT image (if $n < 180$) at the center of a
209 blank background of size 180 by 180 pixels. The baseline CNN was trained from scratch in
210 each condition with 20 million training images and a batch size of 50. To examine the effect
211 of the network size on learnability, we also repeated our experiments with a larger network control
212 (Figure 5, purple curve) with 2 times the number of units in the convolution layers and 4 times the
213 number of units in the fully-connected layers.

214 *Results*

215 In all conditions, we found a strong dichotomy in the observed learning curves. In cases where
216 learning occurred, training accuracy abruptly jumped from chance-level and gradually plateaued.
217 We call this sudden, dramatic rise in accuracy the "learning event". The ATA from a training
218 session was determined by when this sudden rise occurred and at what accuracy it plateaued.
219 When there was no learning event, accuracy remained at chance and ATA was 0.5.

220 In SR, across all image parameters over all random initializations, the learning event immediately
221 occurred at the start of training and quickly approached 100% accuracy, producing consistently
222 high and flat ATA curves (Figure 5, blue dotted lines). In SD, however, we found that ATA
223 was overall significantly lower than SR even though the training images have been sampled from
224 the same distribution. Additionally, we observed a significant straining effect from one image
225 parameter, image size (n). Increasing image size progressively decreased ATA by making learning
226 event progressively less likely (Figure 5, red dotted lines): the network learned SD in 7 out of 10
227 random initializations for the baseline parameter configuration while it only learned it in 4 out of 10
228 on 120×120 images. At image size 150×150 and above, the network never learned the problem.
229 Increasing the number of items produced a slightly different straining effect. While the frequency
230 at which learning event occurred did not change significantly, the final accuracy reached by the
231 end of training steadily decreased from over 90% to around 80%. In contrast, increasing item size
232 produced no visible straining effect on the CNN. Similar to SR, learnability, both in terms of the
233 frequency of learning event as well as final accuracy, did not change significantly over the range
234 of item sizes we considered. Using a CNN with more than twice the number of free parameters
235 as a control did not change the qualitative trend observed in the baseline model (Figure 5, purple
236 dotted lines).

237 We hypothesize that these straining effects reflect the way image size contributes to image
238 variability. A little arithmetic shows that image variability is an exponential function of image
239 size as the base and number of items as the exponent. Thus, increasing image size while fixing the
240 number of items at 2 results in a quadratic-rate increase in image variability, while increasing the

241 number of items leads to an exponential-rate increase in image variability. Image variability is also
242 an exponential function of item size as the exponent and 2 (for using binary pixels) as the base.

243 The comparatively weak effects of item size and item number sheds light on the computational
244 strategy used by CNNs to solve SD. Our working hypothesis is that CNNs learn “subtraction
245 templates”, filters with one positive region and one negative region (like a Haar or Gabor wavelet),
246 in order to detect the similarity between two image regions. A different subtraction template is
247 required for each relative arrangement of items, since each item must lie in one of the template’s
248 two regions. When identical items lie in these opposing regions, they are effectively subtracted
249 by the synaptic weights. This difference is then used to choose the appropriate same/different
250 label. Note that this strategy does not require memorizing specific items. Hence, increasing item
251 size (and therefore total number of possible items) should not make the task appreciably harder.

252 Further, a single subtraction template can be used even in scenes with more than two items, since
253 images are classified as “same” when they have *at least* two identical items. So, any straining
254 effect from item number should be negligible as well. Instead, the principal straining effect with
255 this strategy should arise from image size, which increases the possible number arrangements of
256 items.

257 Taken together, these results suggest that, when CNNs learn a PSVRT condition, they are simply
258 building a feature set tailored to the relative positional arrangements of items in a particular data
259 set, instead of learning the abstract “rule” per se. If a network is able to learn features that capture
260 the visual relation at hand (a feature set to detect *any* pair of items arranged horizontally), then these
261 features should, by definition, be minimally sensitive to the image variations that are irrelevant to

262 the relation. This seems to be the case only in SR. In SD, increasing image variability lowered ATA
263 for the CNNs. This suggests that the features learned by CNN are not invariant rule-detectors, but
264 rather merely a collection of templates covering a particular distribution in the image space.

265 **Experiment 3: Is object individuation needed to solve visual relations?**

266 Our main hypothesis is that CNNs struggle to learn visual relations in part because they are
267 feedforward architectures which lack a mechanism for grouping features into individuated objects.
268 Recently, however, Santoro et al. (2017) proposed the relational network (RN), a feedforward
269 architecture aimed at learning visual relations without such an individuation mechanism. RNs are
270 fully-connected feedforward networks which operate on pairs of so-called “objects” (Figure 6a).
271 These objects correspond to feature columns coarsely sampled at all retinotopic locations from a
272 high-level layer of a CNN (similar, in a sense, to the feature columns found in higher areas of the
273 visual cortex, see Tanaka, 2003).

274 As such, these feature vectors will sometimes represent parts of the background, incomplete
275 items or even multiple items because the network does not explicitly represent individual objects.
276 Santoro et al. (2017) found that an RN architecture substantially outperformed a baseline CNN
277 on various reasoning problems. The authors emphasize that their model performed well even
278 though it employs a highly unstructured notion of object: “A central contribution of this work is
279 to demonstrate the flexibility with which relatively unstructured inputs, such as CNN or LSTM
280 embeddings, can be considered as a set of objects for an RN.”

281 In particular, the RN was able to outperform a baseline CNN on the “sort-of-CLEVR” challenge,
282 a visual question answering task using images with simple geometric items (see Figure 7(a) for

283 examples of sort-of-CLEVR items). In “sort-of-CLEVR”, scenes contain up to six items, each of
284 which has one of two shapes and six colors. The RN was trained to answer both relational questions
285 (e.g., “*What is the shape of the object that is farthest from the gray object?*”) and non-relational
286 questions (e.g., “*Is the red object on the top or bottom of the scene?*”). However, while the authors
287 trained the RN to compare the attributes of scene items (e.g., “*How many objects have the same*
288 *shape as the green object.*”), they did not examine whether the model could learn the concept of
289 sameness, per se (e.g., “*Are any two items the same in this scene?*”). Detecting sameness is a
290 particularly hard task because it requires matching all attributes between all pairs of items.

291 Without testing the RN on this more difficult task, it is difficult to evaluate the efficacy of the
292 model’s “unstructured” objects. If the model learns that an object is a flexible combination of any
293 colors and shapes from its training, then it should be able to detect same-different relations among
294 novel combinations of familiar shapes and colors. That is, it should be able to “group” these item
295 attributes into a new object. If, on the other hand, RN object representations reflect *particular*
296 familiar color-shape combinations, then it would not be able to transfer the concept of sameness to
297 new combinations.

298 To investigate these alternatives, we trained an RN on a two-item same-different task using
299 sort-of-CLEVR items, but leaving out certain color-shape combinations. Furthermore, to examine
300 the efficacy of perceptual grouping on same-different problems, we introduced a novel model
301 which forcibly groups pixels in single items into object representations.

302 Our new model is a “Siamese” network (Bromley et al., 1994) which processes each scene item in
303 a separate (CNN) channel and then passes the processed items to a single classifier network. This

304 idealized model simulates the effects attentional selection and perceptual grouping by segregating
305 the representations of each item. Unlike an RN, whose object representations may in fact contain
306 no item, multiple items or incomplete items, object representations in the Siamese network contain
307 exactly one item.

308 *Methods*

309 **Sub-experiment 3.1: Failure of relational transfer to novel attribute combinations** Here,
310 we sought to measure the ability of an RN to transfer the concept of sameness from a training
311 set to a novel set of objects, a classic and very well-studied paradigm in animal psychology (see
312 Wright and Kelly, 2017; for a review) and thus an important benchmark for models of visual
313 reasoning. We used software for relational networks publicly available at [https://github.](https://github.com/gitlimlab/Relation-Network-Tensorflow)
314 [com/gitlimlab/Relation-Network-Tensorflow](https://github.com/gitlimlab/Relation-Network-Tensorflow). This is essentially the architecture
315 and training procedure used in the original study and we confirmed that this model was able to
316 reproduce the results from (Santoro et al., 2017) on the sort-of-CLEVR task.

317 We constructed twelve different versions of the sort-of-CLEVR dataset, each one missing one of
318 the twelve possible color \times shape attribute combinations, see Figure 7(a). Images in each dataset
319 only depicted two items, randomly placed on a 128×128 background. Half of the time, these
320 items were the same (same color and same shape). For each dataset, we trained the RN architecture
321 to detect the possible sameness of the two scene items while measuring validation accuracy on the
322 left-out images. We then averaged training accuracy and validation accuracy across all of the
323 left-out conditions.

324 **Sub-experiment 3.2: The need for perceptual grouping and object individuation** Here, we
325 introduce a Siamese network which processes scene items individually in separate CNN “channels”
326 (Fig. 6b). First, we split each PSVRT stimulus into several images, each of which contained a
327 single item. These images were then individually processed by two copies of the same network
328 (mimicking, in a sense, the process of sequentially attending to individuated objects). For example,
329 if one stimulus contained two objects in the original PSVRT, our new stimulus would be presented
330 to the Siamese network as two separate images. The scene items retained their original location in
331 each image so that item position varied just as widely as in the original PSVRT. These images were
332 then individually processed by each CNN channel, using the same architecture as in Experiment
333 2. This resulted in two object-separated feature maps in the topmost retinotopic layer (Fig. 6b).
334 These feature maps were then concatenated before being passed to the classifier.

335 This Siamese configuration is essentially an idealized version of the kinds of object representations
336 resulting from psychological processes such as perceptual grouping and attentional selection.
337 Because convolutional layers in this configuration are now constrained to process only one object at
338 a time, regardless of the total number of objects presented in an image, the network can completely
339 disregard the positional information of individual objects and only preserve information about their
340 identities under comparison.

341 *Results*

342 **Sub-experiment 3.1: Relational transfer to novel attribute combinations** From the
343 sort-of-CLEVR transfer task, we found that the RN does not generalize on average to left-out
344 color+shape attribute combinations (Figure 7). Since there are only 11 color+shape combinations

345 in any given setup, the model did not need to learn to generalize across many items if it could
346 simply memorize all combinations of “same” instances. As a result, the RN learned orders of
347 magnitude faster than the CNNs in Experiment 2. However, while the average training accuracy
348 curve (solid red) rose rapidly to around 90%, the average validation accuracy remained at chance.
349 In other words, there was no transfer of same-different ability to the left-out condition, even though
350 the attributes from that condition (e.g., cyan square) were represented in the training set, just not
351 in that combination (e.g., cyan circle and green square) (Figure 7a).

352 **Sub-experiment 3.2: The need for perceptual grouping and object individuation** We ran
353 the Siamese model on the PSVRT tasks, again measuring ATA. The ATA curves for the Siamese
354 network were strikingly different from that of the CNN in Experiment 2 (Figure 8). Barely any
355 straining effect was observed on the SD task, and the model learned within 5M examples across
356 all image size parameters. Since objects are individuated by fiat, the network need not learn all
357 possible spatial arrangements of items. The network must simply learn to compare whichever two
358 items reach the classifier layers through the two CNN channels. This greatly simplifies the SD
359 problem, alleviating straining.

360 Indeed, in informal experiments (data not shown) we found that very shallow Siamese networks
361 (e.g. with one convolutional layer) could still learn SD much faster than baseline CNNs. These
362 results indicate that object individuation makes same-different problems trivially easy. Naturally,
363 we do not intend our Siamese network as a bona fide solution to visual reasoning, but rather as
364 a proof of the efficacy of object individuation in visual reasoning problems. A genuine visual
365 reasoning model would be able to dynamically select and group features in the scene using the
366 mechanisms explored in the Discussion section.

367 **Discussion**

368 Recent progress in computational vision has been significant. Modern deep learning architectures
369 can discriminate between one thousand object categories (He et al., 2015) or identify faces among
370 millions of distractors (Kemelmacher-Shlizerman et al., 2016) at a level approaching – and possibly
371 surpassing that of human observers. While these neural networks do not aim to mimic the
372 organization of the visual cortex in detail, they are at least partly inspired by biology. Modern
373 deep learning architectures are indeed closely related to earlier hierarchical models of the visual
374 cortex albeit with much better categorization accuracy (see Serre, 2015; Kriegeskorte, 2015; for
375 reviews). Further, CNNs have been shown to account well for monkey inferotemporal data (Yamins
376 et al., 2014) and human lateral occipital data (Khaligh-Razavi and Kriegeskorte, 2014; Guclu
377 and van Gerven, 2015). In addition, deep networks have been shown to be consistent with a
378 number of human behaviors including rapid visual categorization (Eberhardt et al., 2016), image
379 memorability (Dubey et al., 2015), typicality (Lake et al., 2015b) as well as similarity (Peterson
380 et al., 2016) and shape sensitivity (Kubilius et al., 2016) judgments.

381 At the same time, there is a growing body of literature highlighting key dissimilarities between
382 current deep network models and various aspects of visual cognition. One prominent example is
383 adversarial perturbation (Goodfellow et al., 2015), structured image distortions that asymmetrically
384 affects CNNs compared to human participants. Although barely perceptible to a human observer,
385 adversarial perturbation renders an image unrecognizable to a CNN, even though the same CNN
386 can correctly recognize the unperturbed image with high confidence. Another example is the poor
387 generalization of CNNs in conditions that are effortless for human observers, such as learning
388 novel object categories with minimal supervision or when the parts of a familiar object are shown

389 in unfamiliar but realistic configurations (Lake et al., 2015a; Saleh et al., 2016; Erdogan and Jacobs,
390 2017). Direct evidence for qualitatively different visual strategies used by humans and CNNs was
391 shown in (Ullman et al., 2016; Linsley et al., 2017).

392 The present study adds to this body of literature by demonstrating feedforward neural networks’
393 fundamental inability to efficiently and robustly learn visual relations. Our results indicate that
394 visual-relation problems can quickly exceed the representational capacity of feedforward networks.
395 While learning feature templates for single objects appears tractable for modern deep networks,
396 learning feature templates for *arrangements* of objects becomes rapidly intractable because of
397 the combinatorial explosion in the requisite number of templates. That notions of “sameness” and
398 stimuli with a combinatorial structure are difficult to represent with feedforward networks has been
399 long acknowledged by cognitive scientists (Fodor and Pylyshyn, 1988; Marcus, 2001). However,
400 this limitation seems to have been overlooked by current computer vision scientists.

401 Compared to the feedforward networks in this study, biological visual systems excel at detecting
402 relations. Fleuret et al. (2011) found that human observers are capable of learning rather
403 complicated visual rules and generalizing them to new instances from just a few training examples.
404 Participants could learn the rule underlying the hardest SVRT problem for CNNs in our Experiment
405 1, problem 20, from an average of about 6 examples. Problem 20 is rather complicated as it
406 involves two shapes such that “*one shape can be obtained from the other by reflection around*
407 *the perpendicular bisector of the line joining their centers.*” In contrast, the best performing
408 CNN model for this problem could not get significantly above chance from one million training
409 examples.

410 This failure of modern computer vision algorithms is all the more striking given the widespread
411 ability to recognize visual relations across the animal kingdom. Previous studies showed that
412 non-human primates (Donderi and Zelnick, 1969; Katz and Wirght, 2006), birds (Daniel et al.,
413 2015; Martinho III and Kacelnik, 2016), rodents (Wasserman et al., 2012) and even insects (Giurfa
414 et al., 2001) can be trained to recognize abstract relations between training objects and then
415 transfer this knowledge to novel objects. Contrast the behavior of these ducklings with the RN
416 of Experiment 3, which demonstrated no ability to transfer the concept of same-different to novel
417 objects (Figure 7) even after hundreds of thousands of training examples.

418 There is substantial evidence that the neural substrate of visual-relation detection depends on
419 re-entrant/feedback signals beyond feedforward, pre-attentive processes. It is relatively well
420 accepted that, despite the widespread presence of feedback connections in our visual cortex, certain
421 visual recognition tasks, including the detection of natural object categories, are possible in the near
422 absence of cortical feedback – based primarily on a single feedforward sweep of activity through
423 our visual cortex (Serre, 2016). However, psychophysical evidence suggests that this feedforward
424 sweep is too spatially coarse to localize objects even when they can be recognized (Evans and
425 Treisman, 2005). The implication is that object localization in clutter requires attention (Zhang
426 et al., 2011).

427 It is difficult to imagine how one could recognize a relation between two objects without spatial
428 information. Indeed, converging evidence (Logan, 1994; Moore et al., 1994; Rosielle et al.,
429 2002; Holcombe et al., 2011; Franconeri et al., 2012; van der Ham et al., 2012) suggests that
430 the processing of spatial relations between pairs of objects in a cluttered scene requires attention,

431 even when individual objects can be detected pre-attentively.

432 Another brain mechanism implicated in our ability to process visual relations is working memory
433 (Kroger et al., 2002; Golde et al., 2010; Clevenger and Hummel, 2014; Brady and Alvarez, 2015).
434 In particular, imaging studies (Kroger et al., 2002; Golde et al., 2010) have highlighted the role of
435 working memory in prefrontal and pre-motor cortices when participants solve Raven’s progressive
436 matrices which require both spatial and same-different reasoning.

437 What is the computational role of attention working memory in the detection of visual
438 relations? One assumption (Franconeri et al., 2012) is that these two mechanisms allow
439 flexible representations of relations to be constructed *dynamically* at run-time via a sequence of
440 attention shifts rather than *statically* by storing visual-relation templates in synaptic weights (as
441 done in feedforward neural networks). Such representations built “on-the-fly” circumvent the
442 combinatorial explosion associated with the storage of templates for all possible relations, helping
443 to prevent the capacity overload associated with feedforward neural networks.

444 Humans can easily detect when two objects are the same up to some transformation (Shepard and
445 Metzler, 1971) or when objects exist in a given spatial relation (Fleuret et al., 2011; Franconeri
446 et al., 2012). More generally, humans can effortlessly construct an unbounded set of structured
447 descriptions about their visual world (Geman et al., 2015). Given the vast superiority of humans
448 over modern computers in their ability to detect visual relations, we see the exploration of
449 attentional and mnemonic mechanisms as an important step in our computational understanding of
450 visual reasoning.

451 **Acknowledgments**

452 The authors would like to thank Drs. Drew Linsley and Sven Eberhardt for their advice, along
453 with Dan Shiebler for earlier work. This research was supported by NSF early career award [grant
454 number IIS-1252951] and DARPA young faculty award [grant number YFA N66001-14-1-4037].
455 Additional support was provided by the Center for Computation and Visualization (CCV) at Brown
456 University. MR is supported by an NSF Graduate Research Fellowship.

457 **References**

- 458 Abadi, M., Barham, P., Chen, J., Chen, Z., Davis, A., Dean, J., Devin, M., Ghemawat, S., Irving,
459 G., Isard, M., Kudlur, M., Levenberg, J., Monga, R., Moore, S., Murray, D. G., Steiner, B.,
460 Tucker, P., Vasudevan, V., Warden, P., Wicke, M., Yu, Y., and Zheng, X. (2016). TensorFlow:
461 A system for large-scale machine learning. In *Proceedings of the 12th USENIX Conference on*
462 *Operating Systems Design and Implementation, OSDI'16*, pages 265–283, Berkeley, CA, USA.
463 USENIX Association.
- 464 Brady, T. F. and Alvarez, G. A. (2015). Contextual effects in visual working memory reveal
465 hierarchically structured memory representations. *J. Vis.*, 15:1–69.
- 466 Bromley, J., Guyon, I., LeCun, Y., Säckinger, E., and Shah, R. (1994). Signature verification using
467 a “siamese” time delay neural network. In *Advances in Neural Information Processing Systems*,
468 pages 737–744.
- 469 Clevenger, P. E. and Hummel, J. E. (2014). Working memory for relations among objects.
470 *Attention, Perception, Psychophys.*, 76:1933–1953.

471 Daniel, T. A., Wright, A. A., and Katz, J. S. (2015). Abstract-concept learning of difference in
472 pigeons. *Anim. Cogn.*, 18(4):831–837.

473 Donderi, D. and Zelnicker, D. (1969). Parallel processing in visual same-different. *Percept.*
474 *Psychophys.*, 5(4):197–200.

475 Dubey, R., Peterson, J., Khosla, A., Yang, M.-H., and Ghanem, B. (2015). What makes an object
476 memorable? In *Proceedings of the IEEE International Conference on Computer Vision*, pages
477 1089–1097.

478 Eberhardt, S., Cader, J. G., and Serre, T. (2016). How deep is the feature analysis underlying rapid
479 visual categorization? In Lee, D. D., Sugiyama, M., Luxburg, U. V., Guyon, I., and Garnett,
480 R., editors, *Advances in Neural Information Processing Systems 29*, pages 1100–1108. Curran
481 Associates, Inc.

482 Ellis, K., Solar-lezama, A., and Tenenbaum, J. B. (2015). Unsupervised Learning by Program
483 Synthesis. *Neural Information Processing Systems*, pages 1–9.

484 Erdogan, G. and Jacobs, R. A. (2017). Visual shape perception as bayesian inference of 3D
485 object-centered shape representations. *Psychol. Rev.*, 124(6):740–761.

486 Evans, K. K. and Treisman, A. (2005). Perception of objects in natural scenes: is it really attention
487 free? *J. Exp. Psychol. Hum. Percept. Perform.*, 31(6):1476–1492.

488 Fleuret, F., Li, T., Dubout, C., Wampler, E. K., Yantis, S., and Geman, D. (2011). Comparing
489 machines and humans on a visual categorization test. *Proc. Natl. Acad. Sci. U. S. A.*,
490 108(43):17621–5.

- 491 Fodor, J. A. and Pylyshyn, Z. W. (1988). Connectionism and cognitive architecture: A critical
492 analysis. *Cognition*, 28(1-2):3–71.
- 493 Franconeri, S. L., Scimeca, J. M., Roth, J. C., Helseth, S. A., and Kahn, L. E. (2012). Flexible
494 visual processing of spatial relationships. *Cognition*, 122(2):210–227.
- 495 Geman, D., Geman, S., Hallonquist, N., and Younes, L. (2015). Visual Turing test for computer
496 vision systems. *Proc. Natl. Acad. Sci. U. S. A.*, 112(12):3618–3623.
- 497 Giurfa, M., Zhang, S., Jenett, A., Menzel, R., and Srinivasan, M. V. (2001). The concepts of
498 'sameness' and 'difference' in an insect. *Nature*, 410(6831):930–933.
- 499 Golde, M., von Cramon, D. Y., and Schubotz, R. I. (2010). Differential role of anterior prefrontal
500 and premotor cortex in the processing of relational information. *Neuroimage*, 49(3):2890–2900.
- 501 Goodfellow, I. J., Shlens, J., and Szegedy, C. (2015). Explaining and harnessing adversarial
502 examples. In *International Conference on Learning Representations*.
- 503 Guclu, U. and van Gerven, M. A. J. (2015). Deep neural networks reveal a gradient in the
504 complexity of neural representations across the ventral stream. *Journal of Neuroscience*,
505 35(27):10005–10014.
- 506 Gülçehre, Ç. and Bengio, Y. (2013). Knowledge Matters : Importance of Prior Information for
507 Optimization. *arXiv Prepr. arXiv1301.4083*, pages 1–12.
- 508 He, K., Zhang, X., Ren, S., and Sun, J. (2015). Delving Deep into Rectifiers: Surpassing

509 Human-Level Performance on ImageNet Classification. *arXiv Prepr. arXiv1502.01852*, pages
510 1–11.

511 Holcombe, A. O., Linares, D., and Vaziri-Pashkam, M. (2011). Perceiving spatial relations via
512 attentional tracking and shifting. *Curr. Biol.*, 21(13):1135–1139.

513 Katz, J. S. and Wirght, A. A. (2006). Same/different abstract-concept learning by pigeons. *J. Exp.*
514 *Psychol. Anim. Behav. Process.*, 32(1):80–86.

515 Kemelmacher-Shlizerman, I., Seitz, S. M., Miller, D., and Brossard, E. (2016). The megaface
516 benchmark: 1 million faces for recognition at scale. In *Proceedings of the IEEE Conference on*
517 *Computer Vision and Pattern Recognition*, pages 4873–4882.

518 Khaligh-Razavi, S.-M. and Kriegeskorte, N. (2014). Deep supervised, but not unsupervised,
519 models may explain IT cortical representation. *PLoS Comput. Biol.*, 10(11):e1003915.

520 Kingma, D. P. and Ba, J. L. (2015). Adam: a method for stochastic optimization. In *International*
521 *Conference on Learning Representations*.

522 Kriegeskorte, N. (2015). Deep neural networks: A new framework for modeling biological vision
523 and brain information processing. *Annu Rev Vis Sci*, 1:417–446.

524 Krizhevsky, A., Sutskever, I., and Hinton, G. E. (2012). ImageNet Classification with Deep
525 Convolutional Neural Networks. *Adv. Neural Inf. Process. Syst.*

526 Kroger, J. K., Sabb, F. W., Fales, C. L., Bookheimer, S. Y., Cohen, M. S., and Holyoak, K. J. (2002).

527 Recruitment of Anterior Dorsolateral Prefrontal Cortex in Human Reasoning: a Parametric
528 Study of Relational Complexity. *Cereb. Cortex*, 12(5):477–485.

529 Kubilius, J., Bracci, S., and Op de Beeck, H. P. (2016). Deep neural networks as a computational
530 model for human shape sensitivity. *PLoS Comput. Biol.*, 12(4):e1004896.

531 Lake, B., Salakhutdinov, R., and Tenenbaum, J. (2015a). Human-level concept learning through
532 probabilistic program induction. *Science*, 350(6266):1332–1338.

533 Lake, B. M., Zaremba, W., Fergus, R., and Gureckis, T. M. (2015b). Deep neural networks predict
534 category typicality ratings for images. In *Proceedings of the 37th Annual Conference of the*
535 *Cognitive Science Society*.

536 LeCun, Y., Bengio, Y., and Hinton, G. (2015). Deep learning. *Nature*, 521(7553):436–444.

537 LeCun, Y., Bottou, L., Bengio, Y., and Haffner, P. (1998). Gradient-based learning applied to
538 document recognition. *Proc. IEEE*, 86(11):2278–2323.

539 Linsley, D., Eberhardt, S., Sharma, T., Gupta, P., and Serre, T. (2017). What are the visual features
540 underlying human versus machine vision? In *IEEE ICCV Workshop on the Mutual Benefit of*
541 *Cognitive and Computer Vision*.

542 Logan, G. D. (1994). Spatial attention and the apprehension of spatial relations. *Journal of*
543 *Experimental Psychology: Human Perception and Performance*, 20(5):1015–1036.

544 Marcus, G. (2001). *The Algebraic Mind: Integrating Connectionism and Cognitive Science*. MIT
545 Press, Cambridge, MA.

546 Martinho III, A. and Kacelnik, A. (2016). Ducklings imprint on the relational concept of “same or
547 different”. *Science*, 353(6296):286–288.

548 Moore, C. M., Elsinger, C. L., and Lleras, A. (1994). Visual attention and the apprehension of
549 spatial relations: The case of depth. *J. Exp. Psychol. Hum. Percept. Perform.*, 20(5):1015–1036.

550 Peterson, J., Abbott, J., and Griffiths, T. (2016). Adapting deep network features to capture
551 psychological representations. In Grodner, D., Mirman, D., Papafragou, A., and Trueswel, J.,
552 editors, *38th annual conference of the cognitive science society*, pages 2363–2368.

553 Rosielle, L. J., Crabb, B. T., and Cooper, E. E. (2002). Attentional coding of categorical relations
554 in scene perception: evidence from the flicker paradigm. *Psychon. Bull. Rev.*, 9(2):319–26.

555 Saleh, B., Elgammal, A., and Feldman, J. (2016). The role of typicality in object classification:
556 Improving the generalization capacity of convolutional neural networks.

557 Santoro, A., Raposo, D., Barrett, D. G. T., Malinowski, M., Pascanu, R., Battaglia, P., and
558 Lillicrap, T. (2017). A simple neural network module for relational reasoning. *arXiv Prepr.*
559 *arXiv1706.01427*.

560 Serre, T. (2015). Hierarchical models of the visual system. In Jaeger, D. and Jung, R., editors,
561 *Encyclopedia of Computational Neuroscience*, pages 1309–1318. Springer New York.

562 Serre, T. (2016). Models of visual categorization. *Wiley Interdiscip. Rev. Cogn. Sci.*, 7(3):197–213.

563 Shepard, R. N. and Metzler, J. (1971). Mental Rotation of Three-Dimensional Objects. *Science*,
564 171(3972):701–703.

565 Stabinger, S., Rodríguez-Sánchez, A., and Piater, J. (2016). 25 years of CNNs: Can we compare
566 to human abstraction capabilities? *ICANN*, 9887 LNCS:380–387.

567 Tanaka, K. (2003). Columns for complex visual object features in the inferotemporal cortex:
568 Clustering of cells with similar but slightly different stimulus selectivities. *Cereb. Cortex*,
569 13(1):90–99.

570 Ullman, S., Assif, L., Fetaya, E., and Harari, D. (2016). Atoms of recognition in human and
571 computer vision. *Proc. Natl. Acad. Sci. U. S. A.*, 113(10):2744–2749.

572 van der Ham, I. J. M., Duijndam, M. J. A., Raemaekers, M., van Wezel, R. J. A., Oleksiak,
573 A., and Postma, A. (2012). Retinotopic mapping of categorical and coordinate spatial relation
574 processing in early visual cortex. *PLoS One*, 7(6):1–8.

575 Wasserman, E. A., Castro, L., and Freeman, J. H. (2012). Same-different categorization in rats.
576 *Learn. Mem.*, 19(4):142–145.

577 Wright, A. A. and Kelly, D. M. (2017). Comparative approaches to same/different abstract
578 concept-learning. *Learn. Behav.*, 45:323–324.

579 Yamins, D. L. K., Hong, H., Cadieu, C. F., Solomon, E. A., Seibert, D., and DiCarlo, J. J. (2014).
580 Performance-optimized hierarchical models predict neural responses in higher visual cortex.
581 *Proc. Natl. Acad. Sci. U. S. A.*, 111(23):8619–8624.

582 Zhang, Y., Meyers, E. M., Bichot, N. P., Serre, T., Poggio, T., and Desimone, R. (2011).
583 Object decoding with attention in inferior temporal cortex. *Proc. Natl. Acad. Sci. U. S. A.*,
584 108(21):8850–8855.

Figures/fig1_horizontal.png

Figure 1. (a) State-of-the-art convolutional neural networks can learn to categorize images (including dog breeds) with high accuracy even when the task requires detecting subtle visual cues. (b) In addition to categorizing visual objects, humans can also perform comparison between objects and determine if they are identical up to a rotation (left). The ability to recognize “sameness” is also observed in other species in the animal kingdom such as birds (right). The geometric figures are adapted from (Shepard and Metzler, 1971), and the image with a duckling is taken with permission from (Martinho III and Kacelnik, 2016).

Figures/svrt_examples.pdf

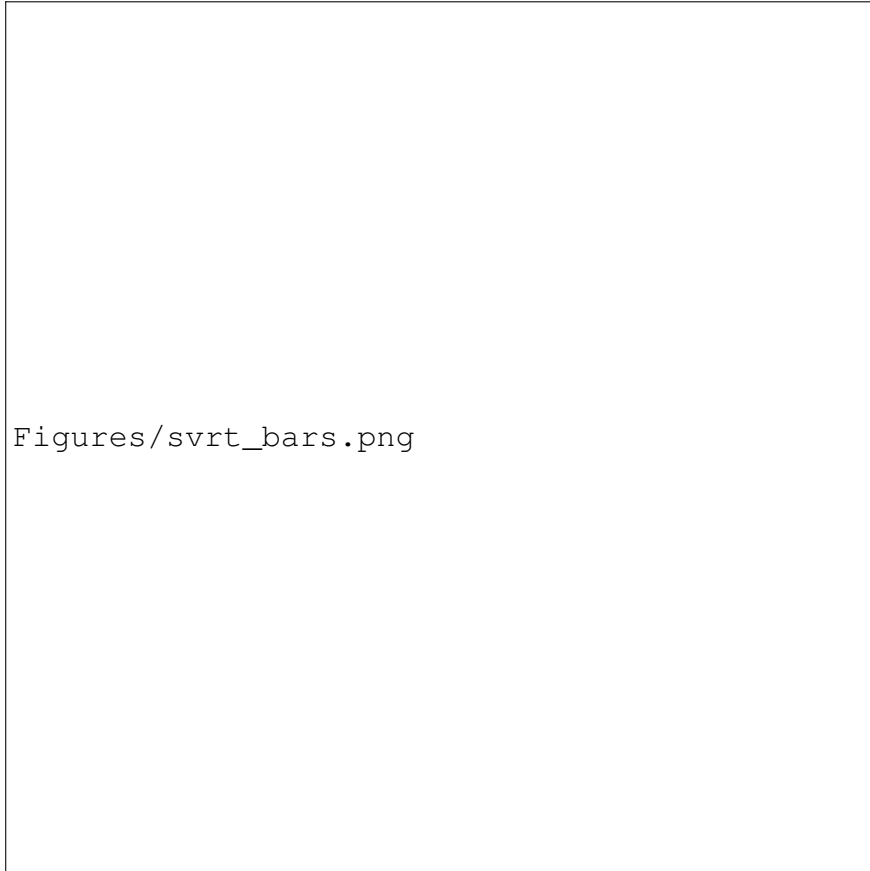
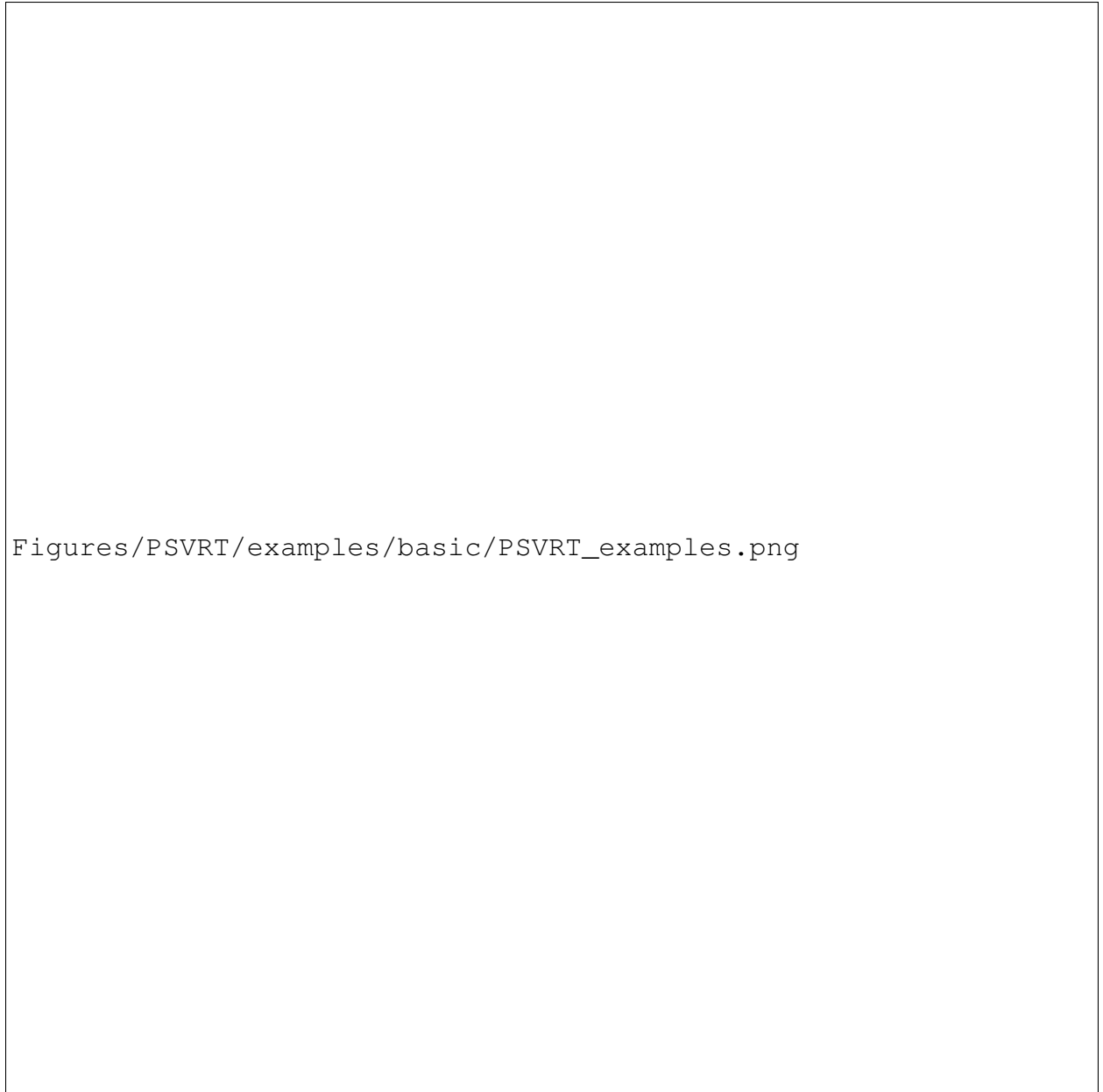


Figure 3. *SVRT results*. Multiple CNNs with different combinations of hyper-parameters were trained on each of the twenty-three SVRT problems. Shown are the ranked accuracies of the best-performing network optimized for each problem individually. The x -axis shows the problem ID. CNNs from this analysis were found to produce uniformly lower accuracies on same-different problems (red bars) than on spatial-relation problems (blue bars). The purple bar represents a problem which required detecting both a same-different relation and a spatial relation.

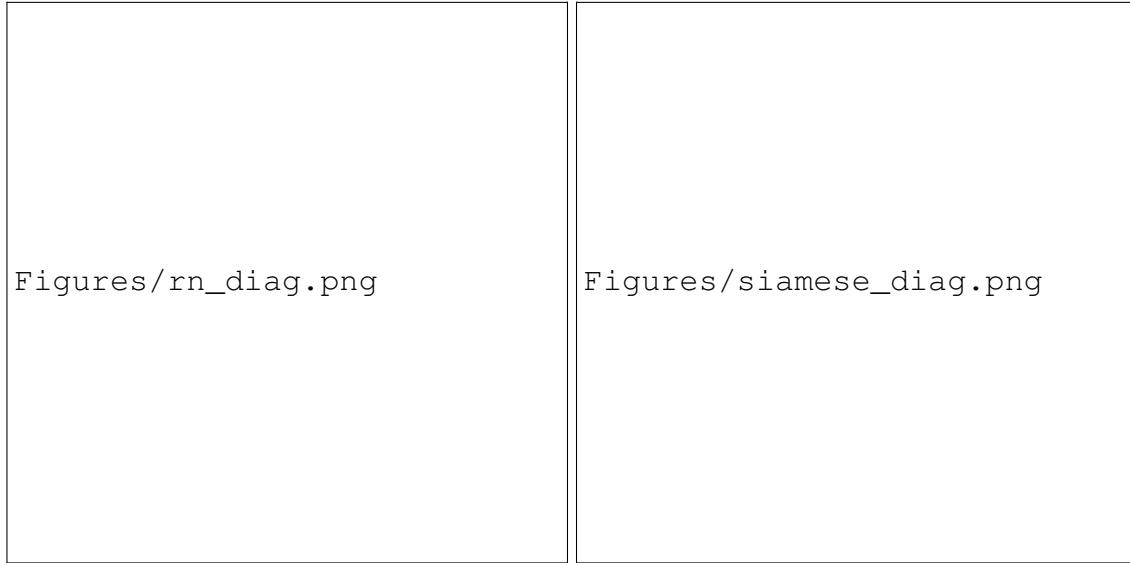


Figures/PSVRT/examples/basic/PSVRT_examples.png

Figure 4. *The PSVRT challenge.* (Left) Four images show the joint categories of SD (grouped by columns) and SR (grouped by rows) tasks. Our image generator is designed such that each image can be used to pose both problems by simply labeling it according to different rules. An image is *Same* or *Different* depending on whether it contains identical (left column) or different (right column) square bit patterns. An image is *Horizontal* (top row) or *Vertical* (bottom row) depending on whether the orientation of the displacement between the items is greater than or equal to 45° . These images were generated with the baseline image parameters: $m = 4$, $n = 60$, $k = 2$. (Right) Six example images show different choices of image parameters used in our experiment: item size, number of items and image size. All images shown here belong to *Same* and *Vertical* categories. When more than 2 items are used, SD category label is determined by whether there are at least two identical items in the image. SR category label is determined according to whether the average orientation of the displacements between all pairs of items is greater than or equal to 45° .

Figures/PSVRT/results/AUC/psvrt_res_horizontal.png

Figure 5. *Average Training Accuracy (ATA) curves over PSVRT image parameters.* ATA denotes the average value of accuracy in each experimental condition measured over the course of 20 million training images and over 10 random initializations. Three curves – SD (red), SD with a large CNN control, (purple) and SR (blue) – are plotted. The three figures display average training accuracy curves over each of three image variability parameters: item size, image size and number of items.



(a)

(b)

Figure 6. *A comparison between a relational network and the proposed Siamese architecture. (a) A relational network (panel (a), top half) is a fully-connected, feedforward neural network which accepts pairs of CNN feature vectors as input. First, the image is passed through a CNN to extract features. Every pair of feature activations (“objects”) at every retinotopic location in the final CNN layer is passed through the RN. The outputs of the RN on every pair of activations is then summed and passed through a final feedforward network, producing the decision. Depending on the spatial resolution of the final CNN layer and the receptive field of each neuron, the object representations of an RN may correspond to a single scene item, multiple items, partial items or even the background. (b) In contrast, objects in our Siamese network are forced to contain a single item. First, we split stimuli into several images, each containing a single item. Then, each of the images is passed through a separate CNN (here, Channel 1 and Channel 2), producing a representation of a single object. These objects are then combined by concatenation into a single representation and passed through a classifier. The network automates the attentional and perceptual grouping processes suspected to underlie biological visual reasoning (see Discussion).*

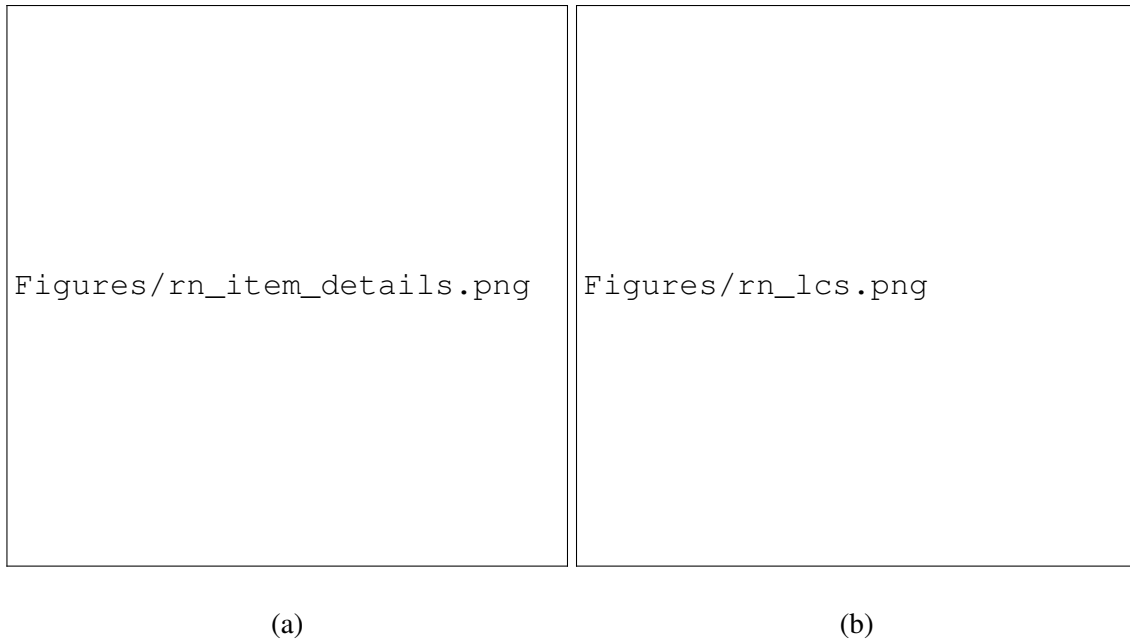


Figure 7. (a) *Sample items used during training and testing in Experiment 3.* We trained relational networks on twelve two-item same-different data sets each missing one color-shape combination from sort-of-CLEVR ($2 \text{ shapes} \times 6 \text{ colors}$). Then, we tested the model on the left-out combination. The top and middle rows of panel (a) show two possible pairs of item when the left-out combination is “cyan square”. Row 1 shows a cyan circle and row 2 shows a green square. However, only in the test set is the model queried about images involving a cyan square (e.g., the “same” image in row 3). Note that, during training, the model observes each left-out attribute, just not in the left-out combination. (b) *Averaged accuracy curves of an RN while being trained on the sort-of-CLEVR data sets missing one color-shape combination.* The red curve shows the training accuracy. The blue dashed line shows the accuracy on validation data with the left-out items.

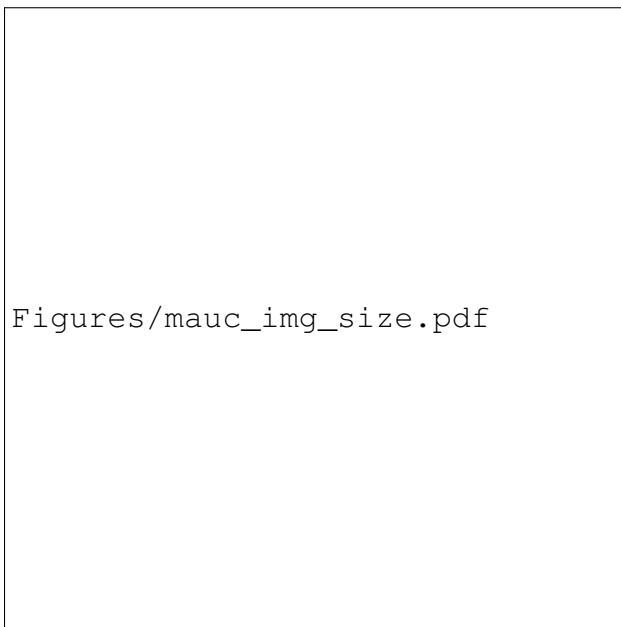


Figure 8. *Average Training Accuracy (ATA) curves for CNN and Siamese model on a two-item same-different (SD) task.* The CNN's ATA curve (red) is taken from Experiment 2. The Siamese network's ATA curve (green) indicates almost no straining. The network learns equally well on large images, for which there is great positional variety of items, as it does on small images, for which there is much less variety.